# The effects of superimposed impulse transients on partial discharge in XLPE cable joint

Wu, Jiayang; Mor, Armando Rodrigo; Smit, Johan J.

**DOI**
10.1016/j.ijepes.2019.03.031

**Publication date**
2019

**Document Version**
Final published version

**Published in**
International Journal of Electrical Power & Energy Systems

Electrical Power and Energy Systems 110 (2019) 497–509

Contents lists available at ScienceDirect

Electrical Power and Energy Systems

journal homepage: www.elsevier.com/locate/ijepes

# The effects of superimposed impulse transients on partial discharge in XLPE cable joint

Jiayang Wu*, Armando Rodrigo Mor, Johan J. Smit

*Delft University of Technology, Electrical Sustainable Energy Department, Mekelweg 4, 2628 CD Delft, the Netherlands*

ARTICLE INFO

*Keywords:*
XLPE cable
Cable accessories
Insulation defects
Partial discharge (PD)
Impulse transients

ABSTRACT

In practice, cross-linked polyethylene (XLPE) power cables can be subjected to alternating voltage with superimposed impulse transients. Such impulse transients may initiate partial discharges (PD) in insulation defects even below AC inception voltage. An initiated PD may persist under AC, which will cause insulation degradation. This paper investigates the PD behavior in MV XLPE cable accessories under impulse transients. Different scenarios of PD behavior are measured, described and analyzed. Based on the results, the effects of impulse transients on PD are summarized.

## 1. Introduction

With their excellent technical properties, cross-linked polyethylene (XLPE) underground cables for all voltage levels of AC are increasingly dominating newly installed cable populations. On the other hand, with long time in service, higher probability of failures arises in the cable systems. Many failures occurring in underground cables are caused by third-party damage [1]. But still, more than half of the failures are caused by internal defects in the cable insulation system, in particular in the cable accessories. This is due to the insulation interfacial defects, which were introduced during installation [2,3]. In practice, impulses caused by switching operations or lightning strikes superimpose on the power frequency AC voltage. At the insulation defects, even PDs are not initiated by operating AC voltage, they might be ignited by impulse transients and keep sustained afterwards. Because of this, PD behaviour under impulse voltage conditions has gained more and more interest.

So far, many researches have studied the effects of standard impulses on the aging process of cable insulation by measuring usual PD parameters such as PD inception voltage (PDIV) and extinction voltage (PDEV). However, not many studies focused on the effects of AC superimposed with impulse transients and PD initiation under these conditions. With PD measurements on XLPE cable pieces with terminations, Abdolall et al. confirm that the PD level did not change after the samples were subjected to switching impulses [4]. However, PD behaviour was observed to be different before and after XLPE cable samples were aged by impulses in [5–7]. The measured PDIV and PDEV decreased with aging by impulses, whilst the PD magnitude increased. Similar influence has been observed in EPR cable insulation under AC voltages with superimposed impulses by Cao et al. [8]. There are also material studies of the PD initiation under pure impulses and AC with superimposed impulse transients. In [9] Densley et al. describe the features of discharges that initiated under impulse. In [10] PDs were measured under AC with superimposed impulse voltage, showing that, PDs initiated by impulses could continue with AC under certain conditions. However, these results are based on polymeric material samples instead of cable samples. Furthermore, up to now, the measured PD are described in a classical way, i.e. by means of phase-resolved PD (PRPD) patterns and usual PD parameters. Time-resolved PD (TRPD) current waveforms were measured under impulses by Zhao et al. [11], which revealed the difference in characteristics of discharges occurring under impulses. However, it was still on material samples.

In order to better understand the PD behaviour in a cable, this paper investigates the characteristics of PD for artificial defects in a MV XLPE cable joint under superimposed impulse transients. A lab-developed PD measurement system is applied to measure PD signals during the impulses. The measured PD signals are analysed and described by PRPD patterns, TRPD pulse waveforms, and usual PD parameters. The obtained PD information describes different scenarios of PD initiation under the impulse, as well as the behaviour of those impulse-initiated PD under AC voltage after the impulses. By interpreting the PD behaviour, the effects of impulse transients on PD are derived and summarized.

## 2. Background theory

There are two necessary conditions for partial discharge inception: a sufficiently high electric field and the presence of a first electron. At the

* Corresponding author.
*E-mail address:* j.wu-3@tudelft.nl (J. Wu).

https://doi.org/10.1016/j.ijepes.2019.03.031
Received 16 November 2018; Received in revised form 30 January 2019; Accepted 13 March 2019
Available online 28 March 2019

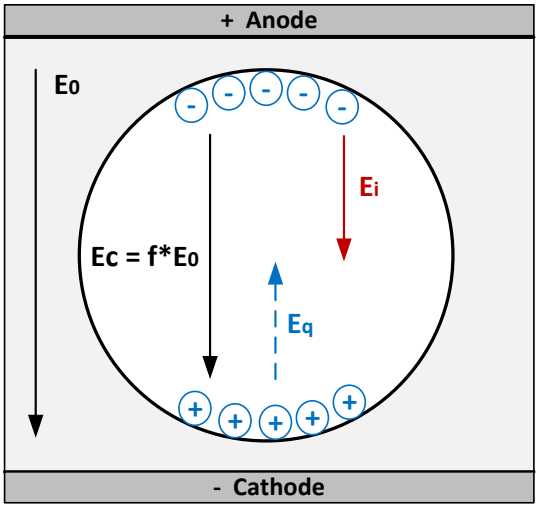


**Fig. 1.** The local field composed of the enhanced background field and the field produced by the surface charges.

defect site there is an enhancement in the electric field which drives the PD occurring. The local enhanced field is composed of two contributing fields [12], as shown in Fig. 1. The first one $E_c$ is an enhancement of the background field $E_0$ inside the insulation, which is caused by the lower permittivity in the defect and the defect shape. The second one $E_q$ is produced by the local space or surface charges $q$ left by the previous PD events. The local field inside the defect is the residual of the two fields, which is expressed as:

$$\vec{E_i} = \vec{E_c} + \vec{E_q} = f \cdot \vec{E_0} + \vec{E_q} \tag{1}$$

$E_i$ is the local field inside the defect which drives PD. $f$ is the field-modification factor that quantifies the field enhancement inside the defect and depends on the relative permittivity of the dielectric and the defect shape [13].

There exists a minimum local field which enables the avalanche and the following partial discharge when a first electron is available. This field is the inception field $E_{inc}$, which corresponds to the PD inception voltage (PDIV). It is associated with the breakdown voltage of the gas in the void, which obeys the Paschen's law. $E_{inc}$ depends on the dimension of the defect (when considering the breakdown voltage of the gas), the pressure and contents in the defect, and the temperature [14]. In a virgin void, the breakdown of the gas is caused by a streamer. The voltage required to start a streamer is usually 5% higher than the voltage corresponding to the Paschen curve [15]. When this void has been aged by discharges for some time, organic acids are produced by chemical reactions in the gas, which will increase the conductivity of the void surface [16]. The conductive part on the surface acts as a cathode, and Townsend discharge can take place. In this case, the inception voltage coincides with the Paschen curve. In other words, $E_{inc}$ in a virgin void is higher than in an aged void.

A first electron is also needed to initiate PD, which is preferably near the cathode so that it can initiate the avalanche travelling towards to the anode [14]. According to Niemeyer [12], there are two main groups of the first electron generation mechanisms: volume generation and surface emission. The volume generation includes the gas ionization by energetic photons due to cosmic and background radiation, and the field detachment of electrons from negative ions. In both cases, the production rate of the first electron depends on the electric field. The surface emission includes the detrapping of electrons from traps on the insulator surface due to field emission from the cathodic conductors, electron release by ion impact, and by the photon effect from both insulating and conducting surfaces.

In the virgin defect where PD has not occurred ever, volume generation is the dominating effect. The first electron will be generated from the cosmic and background radiation, which is a stochastic process. If the first electron is not available yet when the inception voltage has already been reached, then PD will ignite at a field which is higher than the inception field. The waiting time for a first electron in a virgin defect is the PD inception delay time $t_{delay}$. The average $t_{delay}$ depends on the dimensions of the defect, the ionization process and pressure change in the defect, and the ratio of the applied voltage to the inception voltage [12,17], as shown in Eq. (2).

$$t_{delay} = \frac{1}{\dot{N}_e} \approx \frac{1}{\frac{\pi}{6} C_{rad} \varnothing_{rad} \left(\frac{\rho}{p}\right)_0 p l^3 \left(l - \left(\frac{AC}{PDIV}\right)^{-\beta}\right)} \tag{2}$$

wherein, is the rate at which first electrons are produced at the PD site, $C_{rad}$ is the volume ionization parameter and $\varnothing_{rad}$ is the ionizing quantum flux density regarding an air filled void with gas density ρ and pressure $p$, $l$ standing for the void dimension and $\beta$ characterizing the gas combination. PDIV is the PD inception voltage measured without inception delay. With increasing applied AC voltage, $t_{delay}$ decreases.

Once PD has occurred in the defect, the charges produced by the previous PD will be deposited on the insulator surface and in the traps existing on the surface. According to [18], traps with energy depths of the order of eV's are present at the insulator surface. When the charge carriers acquire considerable energy, they can be liberated from the surface and become free electrons [19,20]. The detrapping of electrons from surfaces traps is an additional first electron generation mechanism in the aged defect. The corresponding generation rate in Eq. (2) can be quantified by the surface detrapping phenomena. As a consequence, PDs are ignited with a time lag $t_{lag}$ controlled by surface charge detrapping. The delay caused by detrapping $t_{lag}$ is much lower than that caused by the natural irradiation $t_{delay}$.

The charges deposited directly on the insulator surface from previous PD contribute to the field $E_q$. Those charges have a finite lifetime. They decay after PD events by ion drift and diffusion through the gas, and conducting along the insulator surface [12]. A long decay time means the charges will remain almost intact in the defect and contribute strongly to the $E_q$. The RC decay time constant is of the order

$$\tau_{dc} \sim \frac{\varepsilon_0 r_c}{2\sigma_s} \tag{3}$$

wherein, $\sigma_s$ is the surface conductivity and $r_c$ the equivalent radius of the circumference of the conducting surface. So $\tau_{dc}$ is mainly controlled by the surface conductivity, which depends on the aging state of the defect. In the virgin defect, the surface conductivity of polymers is relatively small, so that the surface charges can survive for a long time. For the aged defect, the surface conductivity becomes increased, so the charges will decay faster. In addition, the conducting surface will shield the defect interior from the electric field, which leads to a suppression of discharges.

Fig. 2 illustrates the electric fields during PD activity. It is hypothesized in Fig. 2a that the first electron is always available and no charge decay is considered. In Fig. 2b, the charge decay is considered. In practice, the statistical characteristics of PDs show strong scatter and variations. PD activities considering the stochastic behaviour of the first electron generation and the charge decay is shown in Fig. 2c.

## 3. Experimental setup

In order to investigate the PD behavior in a MV XLPE cable joint under impulse transient voltages, a test circuit was designed and build up in the HV lab, which enables to supply the impulse transients and to measure PDs during the impulses.

### 3.1. Test circuit

The experimental setup consists of three parts: the generation of AC voltage with superimposed impulse transients, the PD measuring

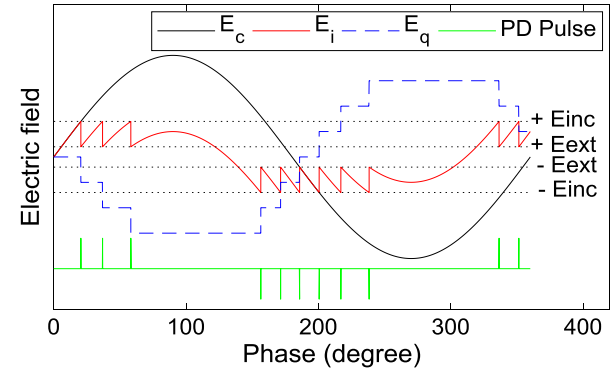


(a). Infinite first electron, no charge decay.

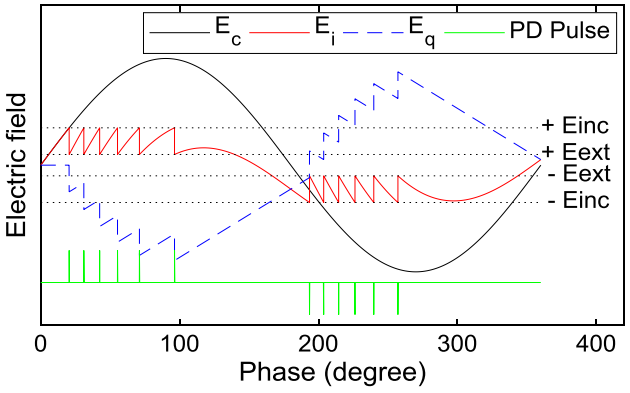


(b). Infinite first electron, charge decay.

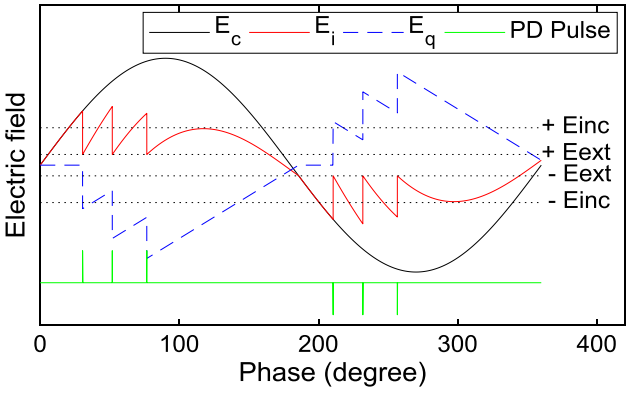


(c). Finite first electron, charge decay.

**Fig. 2.** Electric fields during PD.

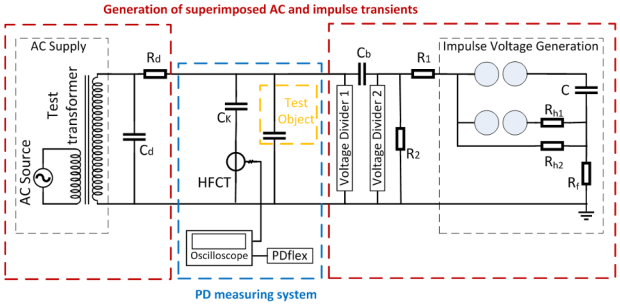


**Fig. 3.** Test circuit.

system, and the test objects. Fig. 3 shows the schematic diagram of the test circuit. $C_d = 2\,\text{nF}$ and $R_d = 4.8\,\text{k}\Omega$ together work as a low pass filter. $C_k = 1\,\text{nF}$ is the coupling capacitor. $C_b = 12.5\,\text{nF}$ serves as a blocking capacitor. And a high voltage divider is used with $R_1 = R_2 = 1\,\text{k}\Omega$.

**Table 1**
Cable samples with defect types.

| Cable sample | Defects | PD |
|---|---|---|
| 1 | Semi-conductive remainder on XLPE surface | No PD |
| | Inserted metal wire which is grounded | PD Type I |
| 2 | Inserted plastic strip with a hole at the edge of the connector | PD Type II |

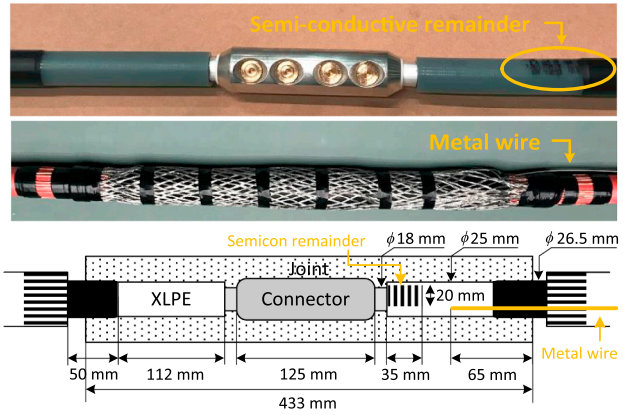


(a). Defect with its dimension and location in cable sample 1.

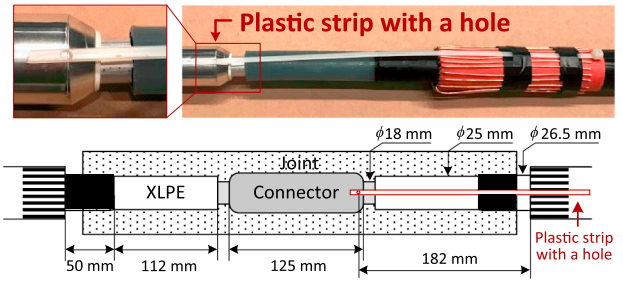


(b). Defect with its dimension and location in cable sample 2.

**Fig. 4.** Cable samples.

### 3.2. Cable and accessories with defects as test objects

Two lengths of 4 m 6/10 kV XLPE cables were used for the experiments, as listed in Table 1. Each cable was assembled with two terminations and a cold shrink cable joint in the middle. Before introducing the artificial defects, both cables were tested as PD free (< 5 pC) up to $3U_0$, namely 18 $kV_{rms}$. Fig. 4 gives the dimensions of the cables, as well as the defects with their dimensions and locations in both cables. In cable sample 1, a small part of the semi-conductive layer was left during peeling, which is a typical defect that can occur in practice when installing cable joints in the field. However, this defect didn't cause PDs in cable sample 1 on short term. Therefore, to simulate aging experimentally, a thin metal wire with diameter of 2 mm was inserted into the cable joint for 65 mm along the interface between the cable and the joint insulation, as shown in Fig. 4a. As a result, PDs of type I were observed in cable sample 1. In cable sample 2, a plastic strip was inserted into the cable joint. A hole with diameter of 2 mm and depth of 1 mm was drilled at one end of the plastic stripe, and the stripe was positioned so that the hole was located at the edge of the connector. This is illustrated in Fig. 4b. By introducing this defect, PDs of type II were observed in cable sample 2.

### 3.3. PD measuring circuit

In this work, the measuring of PD signals was performed continuously during the application of superimposed impulse transients. For this purpose, a measuring system capable of recording and distinguishing between actual PD events and the electromagnetic interferences, noise and disturbances produced together with every firing of impulses was required. To fulfil these constrains, an unconventional PD measuring circuit was preferred over the international standards IEC 60,270 [21] and IEC 60885–3 [22]. The employed measuring system comprises a digital oscilloscope Tektronix DPO7354C, a high frequency current transformer (50 kHz–110 MHz) as a PD sensor and the software PDflex for post processing of data [23]. The results are presented by means of usual PD parameters, PRPD patterns, TRPD waveforms and their frequency spectrum [24–26]. The PD parameters, e.g. charge of PD pulse, are calculated based on the measured PD current by the method described by Mor et al. [25].

### 3.4. Testing voltage

Partial discharges were measured in the cable samples under pure AC voltages as well as AC with superimposed impulse transients. Fig. 5a shows the impulse and the superimposed transient waveforms. Several studies have established that naturally occurring transient voltages do not always resemble the lightning or switching impulse wave shape [27]. In this study, an impulse with a front time of 2.8 μs and a falling time of 526 μs was used to be superimposed on the AC voltage at the peak of the positive half cycle. The testing voltage with the testing procedure is given in Fig. 5b. The AC voltage value was determined to be below the inception value and above the extinction value. The impulses were applied on the AC voltage at the peak with a rate of two impulses per minute. That is, the time interval between two consecutive impulses was around 30–35 s. Before the first impulse, the test object was subjected to only the AC voltage for several minutes to confirm that PD did not occur at the AC voltage level.

## 4. Partial discharge under ac and impulse transient voltage

### 4.1. PD under pure ac voltage

The prepared cable samples were firstly subjected to pure AC voltage to check the PD raised at the artificial defects. After insertion of the thin metal wire PD type I were detected in cable sample 1. Fig. 6a shows the PRPD pattern of the detected PDs at AC of 17 $kV_{pk}$, which is in accordance with a phase-resolved pattern of internal discharges in

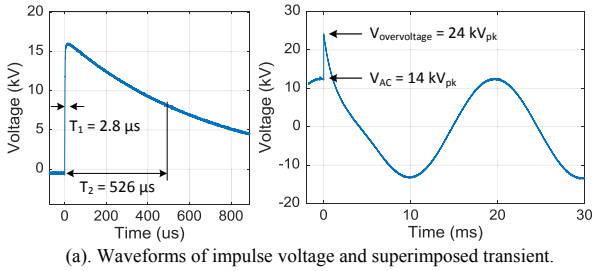


(a). Waveforms of impulse voltage and superimposed transient.

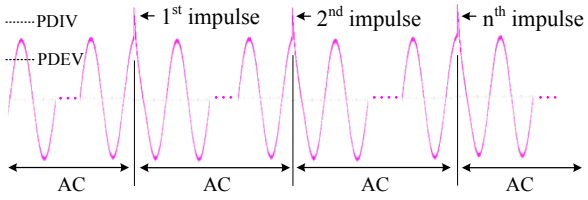


(b). Waveform of testing voltage

**Fig. 5.** Generated transient voltage and testing voltage.

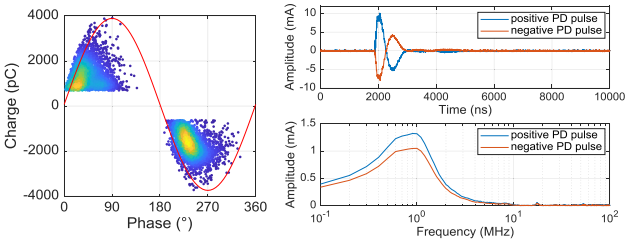


(a). PRPD pattern. (b). TRPD pulse shape and frequency spectrum.

**Fig. 6.** Characteristics of PD type I in cable sample 1 at 17 $kV_{pk}$.

square cavity, given by Gulski in [28]. There might be different reasons causing cavities in cable sample 1. By inserting the metal wire, the sharp tip of the wire can make a scratch on the XLPE surface. Moreover, there might be an air gap existing in the vicinity of the wire tip. All these can lead to internal discharge. TRPD pulse shapes of two PD pulses with opposite polarities with their frequency spectra are given in Fig. 6b. The frequency spectrum shows a peak at 900 kHz. For all the acquired PD pulses, their peak frequencies locate in the range of 800 kHz to 1 MHz. This is the characteristic frequency spectrum of the discharges occurred in cable sample 1, which is determined by both the discharges and the test circuit.

PD type II was detected in cable sample 2. With increasing AC voltage on the cable sample, discharges firstly initiated at the negative cycle with inception voltage of 8.6 $kV_{pk}$. Fig. 7a shows the PRPD pattern and TRPD pulse shape with its peak frequency of 1 MHz at an AC voltage of 9.2 $kV_{pk}$. By further increasing the voltage, discharges started to initiate at the positive cycle with inception voltage of 14.5 $kV_{pk}$. Fig. 7b shows this case at an AC voltage of 17 $kV_{pk}$. PD type II behaves like the discharges in an electrode-bounded cavity, described by Gulski [28], which is characterized by a significant difference between the positive half and the negative half of the voltage cycle [29]. The electrode-bounded cavity was created by the hole on the plastic strip, which is bounded with the connector.

### 4.2. PD under impulse transients

The cable samples were then subjected to the testing voltage waveforms as shown in Fig. 5. Before each test, PDIV and PDEV values were firstly measured. Two parameters are defined to describe the characteristics of the applied impulse transients, as given in Eqs. (4) and

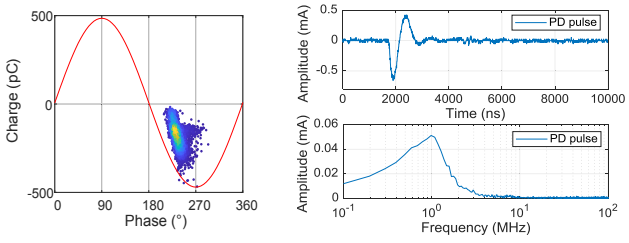


(a). PRPD pattern, TRPD pulse shape and frequency spectrum at 9.2 $kV_{pk}$.

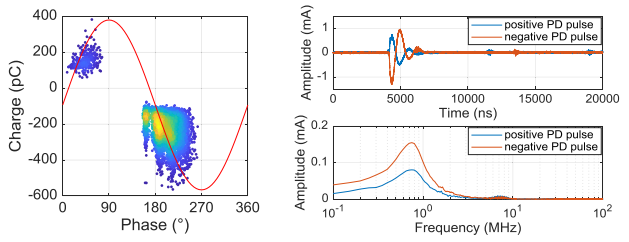


(b). PRPD pattern, TRPD pulse shape and frequency spectrum at 17 $kV_{pk}$.

**Fig. 7.** Characteristics of PD type II in cable sample 2.

**Table 2**
PD tests under testing voltages of impulse transients.

| Test | Cable sample | Test order | Defect Status | PDIV [$kV_{pk}$] | PDEV [$kV_{pk}$] | Testing voltages of impulse transients | | | | | | PD |
|---|---|---|---|---|---|---|---|---|---|---|---|---|
| | | | | | | Label | AC [$kV_{pk}$] | Overvoltage [$kV_{pk}$] | Amount of impulses | α | β | |
| 1 | 1 | 1 | Virgin | 15.6 | 12.7 | $TV_1$ | 14.1 | 23.4 | 4 | 0.50 | 1.66 | No PD |
| 2 | 1 | 4 | Virgin | 16.1 | 9.9 | $TV_2$ | 15.8 | 27.3 | 20 | 0.05 | 1.73 | |
| 3 | 1 | 3 | Virgin | 16.3 | 11.6 | $TV_3$ | 8.5 | 25.5 | 10 | 1.60 | 3.11 | PD initiate only at the impulse |
| 4 | 2 | 8 | Virgin | 8.6 | 8.2 | $TV_4$ | 8.3 | 14.7 | 10 | 0.75 | 1.77 | periods |
| 5 | 1 | 5 | Virgin | 16.1 | 10.6 | $TV_5$ | 15.7 | 25.0 | 14 | 0.10 | 1.59 | PD initiate only at AC after the |
| 6 | 1 | 6 | Aged | 13.3 | 11.0 | $TV_6$ | 12.7 | 24.2 | 1 | 0.30 | 1.91 | impulses |
| 7 | 1 | 2 | Virgin | 16.3 | 10.6 | $TV_7$ | 15.7 | 27.2 | 10 | 0.10 | 1.73 | PD initiate at the impulse |
| 8 | 1 | 7 | Aged | 12.3 | 11.46 | $TV_{81}$ | 11.6 | 23.0 | 37 | 0.80 | 1.98 | moment and persist at the AC |
| | | | | | | $TV_{82}$ | 11.9 | 23.4 | 20 | 0.50 | 1.97 | |
| | | | | | | $TV_{83}$ | 12.2 | 23.8 | 20 | 0.10 | 1.95 | |
| | | | | | | $TV_{84}$ | 12.4 | 24.1 | 20 | −0.10 | 1.94 | |
| | | | | | | $TV_{85}$ | 12.7 | 24.5 | 11 | −0.50 | 1.93 | |

(5). The ratio $\alpha$ describes the relation between the applied AC voltage and PDIV/PDEV. The ratio $\beta$ is the superimposed overvoltage peak divided by the applied AC voltage peak value.

$$\alpha = \frac{PDIV - AC}{PDIV - PDEV} \tag{4}$$

$$\beta = \frac{Overvoltage_{peak}}{AC_{peak}} \tag{5}$$

When the AC voltage is below PDIV and above PDEV, $\alpha$ is a positive value below 1. The closer that AC is to PDIV, the smaller value $\alpha$ has. When AC is below PDEV, $\alpha$ becomes larger than 1. If AC is higher than PDIV, then $\alpha$ turns to negative. The impulse voltages were set mostly with certain peak values so that the obtained transients had the overvoltage ratio $\beta$ in the range of 1.7–2.0, which could happen in practice. Moreover, for all the defined testing voltages, the time period of transient overvoltage being higher than PDIV due to the impulse application is long enough for PD to occur.

Table 2 lists the PD tests under the designed testing voltages of impulse transients. For each test, the used cable sample with its defect status and its PDIV and PDEV are shown. The cable samples are regarded as in virgin statuses when the PDIV keeps the same value as it is measured in a virgin sample for the very first time. When the PDIV gets decreased, then the cable samples are regarded as aged statuses. The applied testing voltage is then described by its AC and overvoltage peak values, $\alpha$ and $\beta$, and the number of impulses contained in the testing voltage. Different scenarios of PD behaviour under impulse transients have been observed, which will be described in the following sections.

#### 4.2.1. No PD being triggered by impulse transients

With the application of impulses, it happened that no PD occurred during the testing process, see test 1 and test 2.

#### 4.2.2. PD initiate only in the impulse period

We define the impulse period as one 50 Hz cycle, i.e. 20 ms, counting from the very start of the superimposed impulse transient. In test 3 and 4, it was successful to observe PD occurring in the cable samples after applying the impulses. All the observed PDs occurred only in the impulse periods. After that, PD did not occur anymore with AC voltage.

In test 3, PD only occurred instantaneously in the impulse periods of all the applied 10 impulses, except for the 2nd impulse, shown in Fig. 8. Each dot represents one PD pulse. The red lines indicate the impulses. Fig. 9 illustrates the PD initiation under the 1st impulse. A discharge of larger magnitude occurred near the peak of the impulse. This is referred as the main discharge [10]. A discharge of smaller magnitude with opposite polarity occurred near to the beginning of the negative cycle. This is referred to the reverse discharge. After the two discharges, PD extinguished. The TRPD pulse shapes and the frequency spectra after the impulse are given in Fig. 10, which are similar to the PD pulses measured under pure AC, shown in Fig. 6. We can hereby recognize the instantaneous PD initiated by the impulse as the discharge type I in cable sample 1. In this test, the occurrence of PD is highly correlated with the application of impulses, instead of being sustained by the AC voltage.

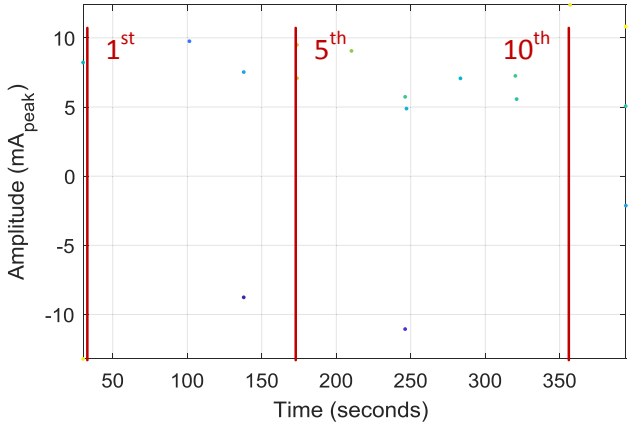


**Fig. 8.** Test 3: PD occurred at impulse moments.

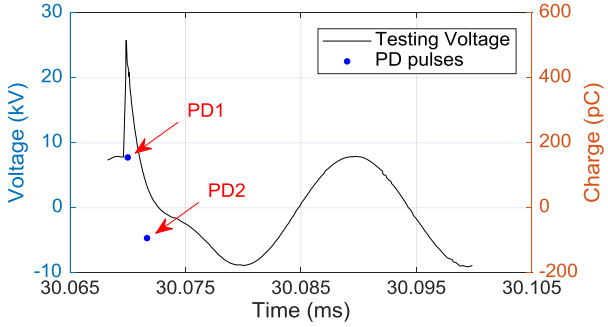


**Fig. 9.** Test 3: PD pulses occurred at 1st impulse moment.

Similar phenomenon was observed with cable sample 2 in test 4, shown in Figs. 11–13. The AC level of the testing voltage $TV_4$ was determined based on the inception and extinction values of discharges occurred at negative cycle. There were PD occurring at every impulse moment. However, no PD was observed near the peak of the impulse. Instead, one or two PD occurred at the negative cycle during the impulse period, as shown in Fig. 12. Then they extinguished. The TRPD pulse shape and the frequency spectrum in Fig. 13 conform well with

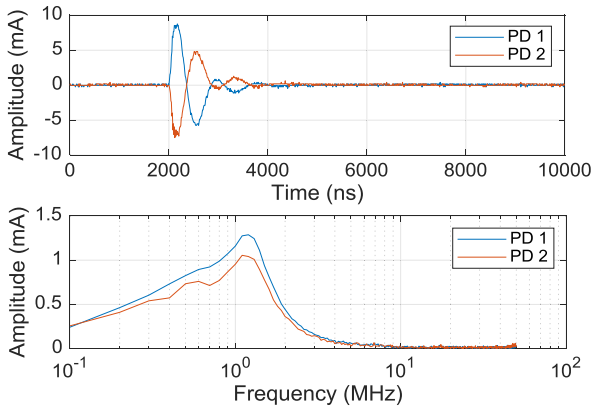


**Fig. 10.** Test 3: TRPD pulse shape and frequency spectrum of PD pulses occurred at 1st impulse moment.

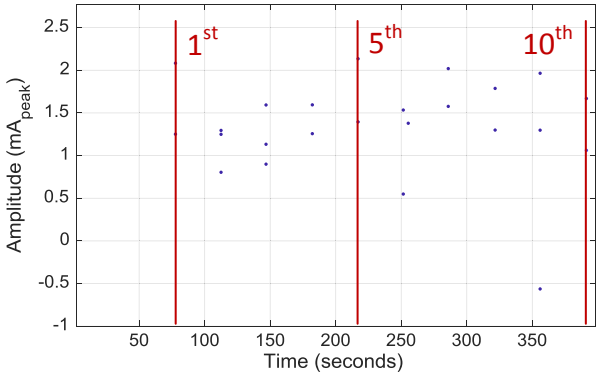


**Fig. 11.** Test 4: PD occurred at impulse moments.

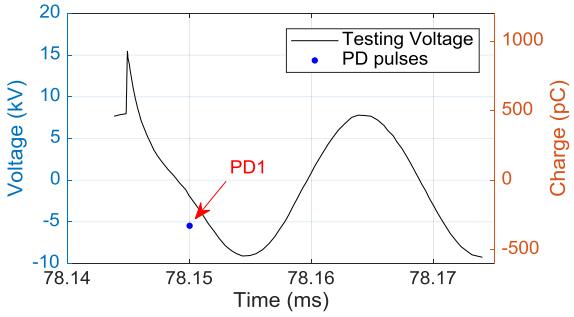


**Fig. 12.** Test 4: PD pulses occurred at 1st impulse moment.

discharge type II that was measured for cable sample 2 under pure AC.

*4.2.3. PD initiate only at AC after the impulse*

In some cases, PD did not initiate in the impulse period, but at the AC voltage after the impulse. This phenomenon was observed in test 5 and test 6.

In test 5, no PD were detected in cable sample 1 during the application of 14 impulses. However, PD initiated under AC when the impulses were gone, shown in Fig. 14 as the cluster after the 14th impulse. The PRPD, given in Fig. 15a, further proves that the occurred discharges were sustained by the AC voltage rather than being initiated by the impulses. Fig. 15b gives typical TRPD pulse shapes and their frequency spectrum, which confirm with that in Fig. 6b.

In test 6, cable sample 1 has encountered only one impulse. PD didn't initiate in the impulse period, but under the AC after the impulse. They persisted actively with the AC. This is shown in Figs. 16 and 17. PRPD pattern, TRPD pulse shapes and frequency spectrum in Fig. 18 confirm the observed PD being the type I discharges characteristic for

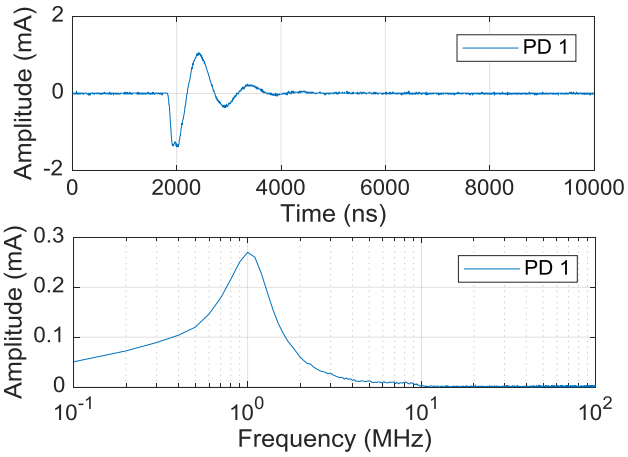


**Fig. 13.** Test 4: TRPD pulse shape and frequency spectrum of PD pulses occurred at 1st impulse moment.

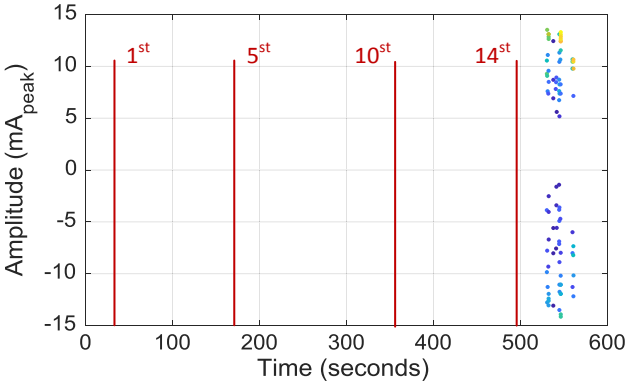


**Fig. 14.** Test 5: PD occurred after 14 impulses.

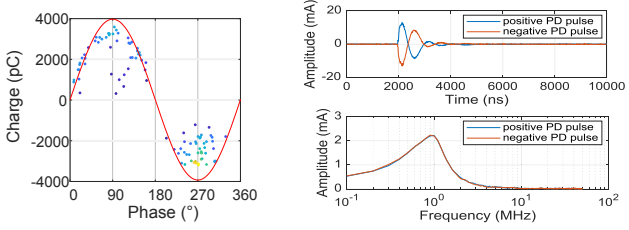


(a). PRPD pattern. (b). TRPD pulse shape and frequency spectrum.

**Fig. 15.** Test 5: Characteristics of PD in cable sample 1.

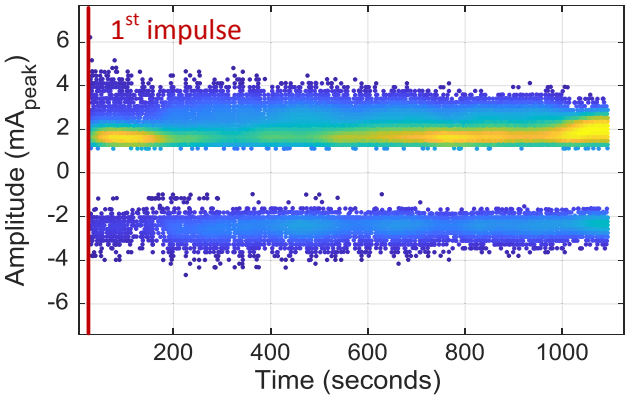


**Fig. 16.** Test 6: PD triggered by one impulse.

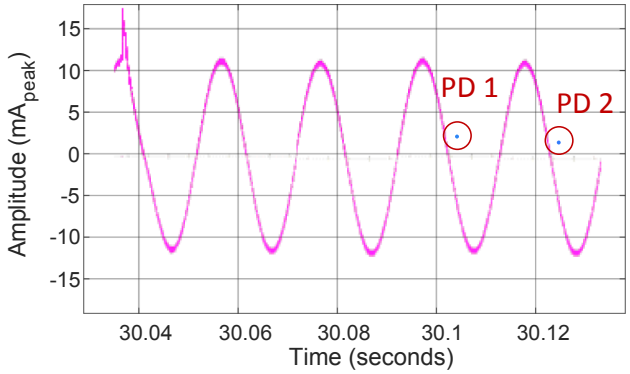


**Fig. 17.** Test 6: PD occurred after 1st impulse.

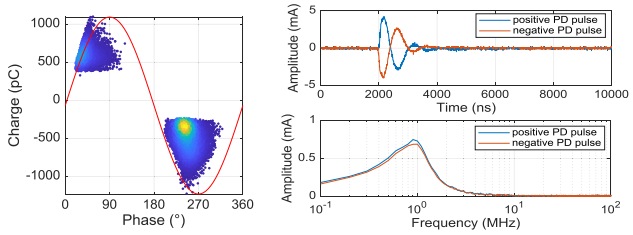


(a). PRPD pattern.

(b). TRPD pulse shape and frequency spectrum.

**Fig. 18.** Test 6: Characteristics of PD in cable sample 1.

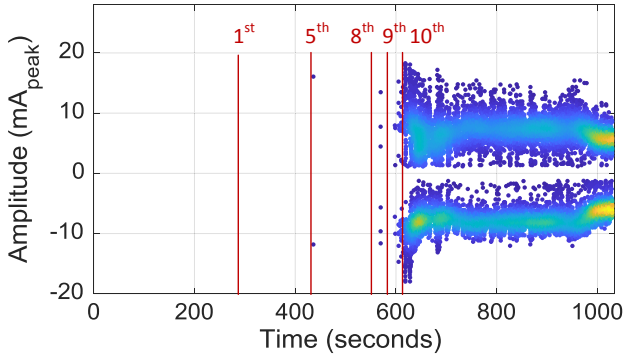


**Fig. 19.** Test 7: PD initiation with consecutive impulses.

cable sample 1.

### 4.2.4. PD initiate in the impulse period and persist at AC

PD initiated by the impulses can also persist under the AC voltage after the impulses have gone. This phenomenon was observed in test 7 and test 8.

In test 7, no PD initiated before the 5th impulse. When the 5th impulse was applied, two PD initiated in the impulse period and then extinguished, as shown in Fig. 20. After the 8th and 9th impulses, more PD initiated, recurred and extinguished. After the 10th impulse, PD initiated and then became sustained by the AC voltage. This process is shown in Fig. 19. Fig. 21 gives the TRPD and frequency spectrum. PRPD patterns of PD occurred after 5th, 8th, 9th and 10th impulses are shown in Fig. 22.

In test 8, five sets of testing voltages were applied to cable sample 1 uninterruptedly. The AC voltage levels of $TV_{81}$, $TV_{82}$ and $TV_{83}$ were set below PDIV, whilst the AC voltage levels of $TV_{84}$ and $TV_{85}$ were set higher than PDIV. Fig. 23 shows the PD measurements under the five testing voltages.

In this test, PD always initiated in the impulse periods. However, PDs behaved differently under the different AC voltages of different

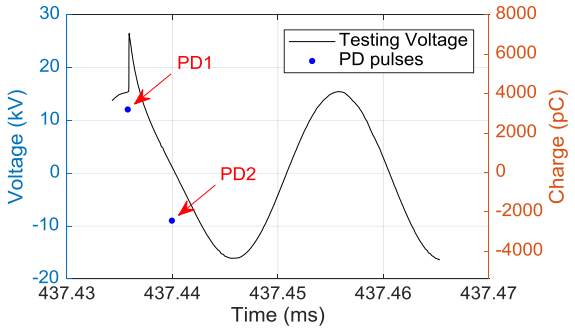


**Fig. 20.** Test 7: PD pulses occurred at 5th impulse moment.

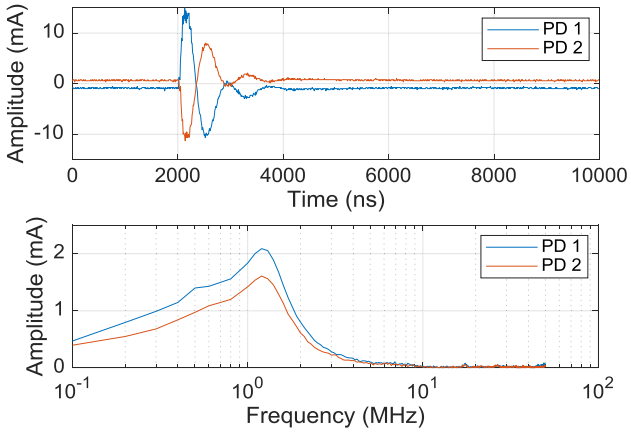


**Fig. 21.** Test 7: TRPD pulse shapes and frequency spectrum.

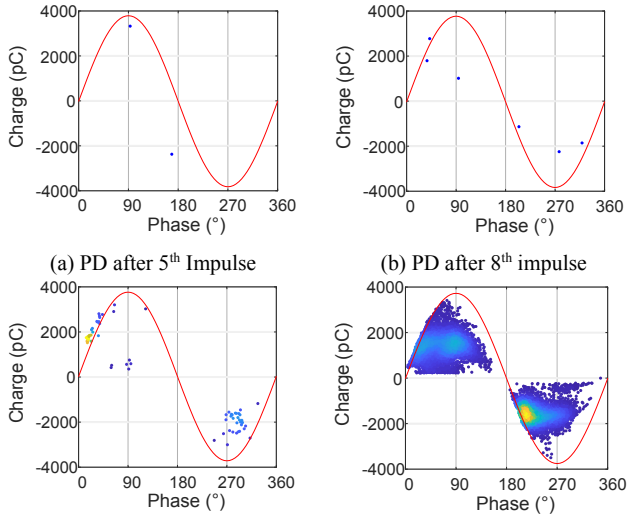


(a) PD after 5th Impulse

(b) PD after 8th impulse

(c) PD after 9th Impulse

(d) PD after 10th Impulse

**Fig. 22.** Test 7: PRPD patterns of PDs after 5th, 8th, 9th and 10th impulses.

testing voltages. Under $TV_{81}$, PDs were initiated by each impulse and lasted for a couple of seconds, then they stopped. Several seconds later, they recurred again for a short time, and so forth. This is shown in Fig. 23b. Such an intermittent PD behaviour was also observed under $TV_{82}$, shown in Fig. 23c. Under $TV_{83}$, the same intermittent behaviour was observed for the first six impulses. After the 6th impulse, PD occurred more continuously and extensively, and became sustained at last, as shown in Fig. 23d. Under $TV_{84}$ and $TV_{85}$, PDs were occurring sustainably. All the PRPD patterns confirm the PDs to be the type I discharge from cable sample 1.

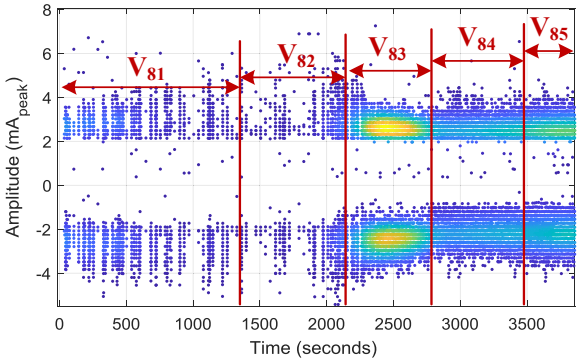


(a). PD under five sets of testing voltage $TV_{81}$ to $TV_{85}$.

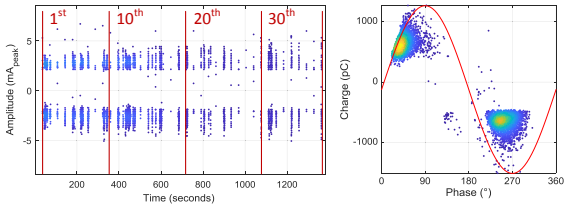


(b). PD under testing voltage $TV_{81}$.

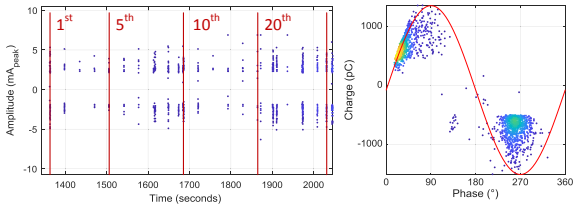


(c). PD under testing voltage $TV_{82}$.

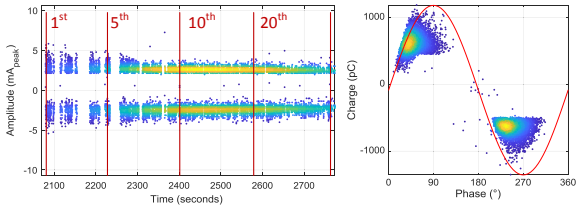


(d). PD under testing voltage $TV_{83}$.

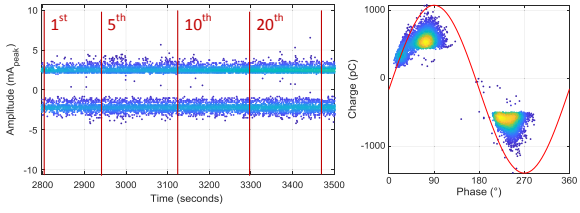


(e). PD under testing voltage $TV_{84}$.

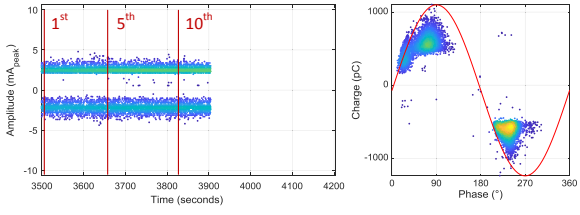


(f). PD under testing voltage $TV_{85}$.

**Fig. 23.** Test 8: PD initiation and development with impulses.

## 5. The effects of impulse transients on partial discharge

The difference in PD behavior under impulse transients are related to the local electric field condition and the charges in the defects, as well as the aging status of the insulation. In the next, the mechanism of different scenarios are clarified.

### 5.1. No PD being initiated by impulse transients

The time to breakdown in the gas is in the order of μs for the Townsend mechanism and 1–100 ns for the streamer mechanism [30]. In all the tests, the time period of the superimposed transient overvoltage being higher than PDIV was 1–2 ms on average. In this case, both the time period and the electric field during the overvoltage period were large enough to initiate PD. However, no PD was observed in test 1 and test 2. We can hereby infer that the first electron was not present during the entire test. Since the cable sample was discharged after each test, the surface and space charges flow away. Such a long inception delay is due to the stochastic generation of an electron by cosmic and background radiation.

### 5.2. PDS initiate only in the impulse period

In test 3, a positive main discharge initiated at the impulse rising phase, then a negative reverse discharge occurred near but below voltage zero, see Fig. 9. Afterwards PD extinguished. It is necessary to notice that, the negative reverse discharge occurred at a field that is below the extinction field. This phenomenon can be explained based on the model shown in Fig. 24 and the field conditions shown in Fig. 25.

Fig. 24a shows how the fields change during the 1st impulse period. $E_c$ is an enhancement of $E_0$, where $E_0$ is generated by the applied testing

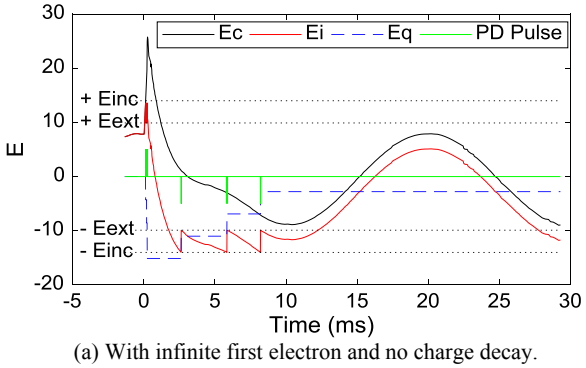


(a) With infinite first electron and no charge decay.

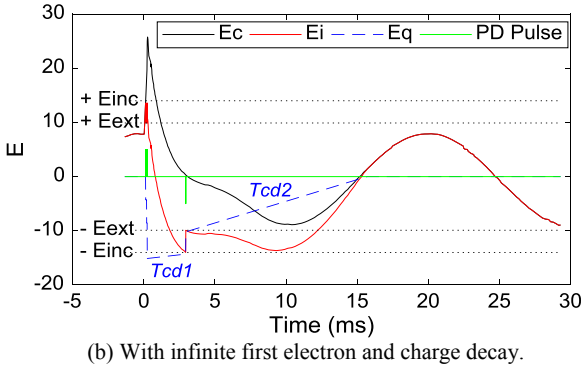


(b) With infinite first electron and charge decay.

**Fig. 24.** The field changes after 1st impulse in test 3.

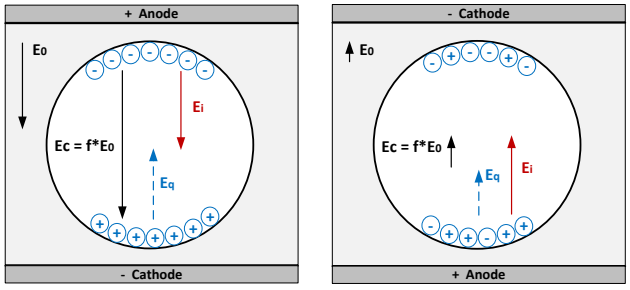


(a). After the positive PD, $E_c$ and $E_i$ in positive polarity.

(b). After the negative PD, $E_c$ and $E_i$ in negative polarity.

**Fig. 25.** Field conditions in the void during PD process in test 3.

voltage $TV_3$. Thus, $E_c$ follows the wave shape of $TV_3$. $E_q$ is created by the surface charges. The residual local field $E_i$ is contributed by $E_c$ and $E_q$, which drives PD occurrence. It is assumed that the first electron is always available and there is no charge decay. In this case, the main discharge ignites as soon as the local field $E_i$ reaches the inception field $E_{inc}$ at the impulse rising phase. During the discharge process, charges from the discharge are accumulated on the insulation surface, which leads to an increasing $E_q$. Correspondingly, $E_i$ reduces until it reaches the extinction field $E_{ext}$. At this moment, discharge extinguishes, $E_q$ stops increasing and then keeps unchanged since there is no charge decay. The field condition is shown in Fig. 25a. Afterwards, $E_i$ changes with $E_c$ until it reaches $-E_{inc}$, then a negative discharge ignites. The charges deposited on the surface by the negative discharge have an opposite polarity with the existing charges, which reduce $E_q$. The field condition now is shown in Fig. 25b. After the negative discharge, $E_i$ retraces $E_c$. As a result, the negative PDs would recur periodically.

If considering the charge decays, expressed by the decay time constant $\tau_{cd}$, the phenomenon will change as shown in Fig. 24b. Between two PD events, the charges decay with a certain $\tau_{cd}$, so the field $E_q$ generated by the charges decreases. A smaller $\tau_{cd}$ means a faster charge decay and a faster change of $E_q$. After the positive discharge, the charges start to decay slowly with a large $\tau_{cd1}$. $E_q$ hereby decreases slightly. After the negative PD, due to the damage of the previous discharge, the surface conductivity may become larger, which lead to a smaller $\tau_{cd2}$ and faster decay. Moreover, the polarity of $E_c$ reverses now, and most positive charges are accumulated at the anode side. As a result, a relatively large $E_i$ with negative polarity is formed, see Fig. 25b. And the surface charges are easy to drift with $E_i$, which means the charges decay faster. With this $\tau_{cd2}$, $E_i$ is unable to reach $E_{inc}$ again and at last converges to $E_c$. Therefore, PD cannot be ignited any more, and there are only two PD events occurring after the impulse, which conforms to the measurement result shown in Fig. 9.

In test 4, discharges only occurred at the negative cycle after the impulse during the impulse period, see Fig. 12. This phenomenon is probably due to the change in $E_q$ caused by the defect. In cable sample 2, the defect was made next to the metal connector. Therefore, a cavity with metal as wall on one side and insulator as wall on the other side was formed. When electric field is present, electrons can overcome the potential barrier to leave the metal into the dielectric and contribute to space charges. Under pure AC, electrons are injected from and gather near the metal wall. On the insulator wall, there are charges deposited in the traps. All these form an electric field in the direction from metal to insulator wall, shown as $E_{q0}$ in Fig. 26. With $E_{q0}$, $E_i$ has a negative offset from $E_c$. This is the reason why the inception voltage in negative cycle is lower than that in positive cycle for cable sample 2, shown in Table 2. When the impulse is applied, the high electric field may cause more electrons being injected from the metal surface and some deposited charges escaping from the traps in the insulator surface. This process will lead to an enhanced $E_{q1}$. Due to the relatively high PDIV for positive cycle, the resulting $E_i$ is not sufficient to ignite PD near the impulse, but it exceeds the PDIV for negative cycle. Consequently, a discharge occurs. With considering the charge decay, $E_q$ returns to $E_{q0}$ after the discharge. Since $E_i$ with offset of $E_{q0}$ doesn't exceed the negative PDIV again, PD extinguishes.

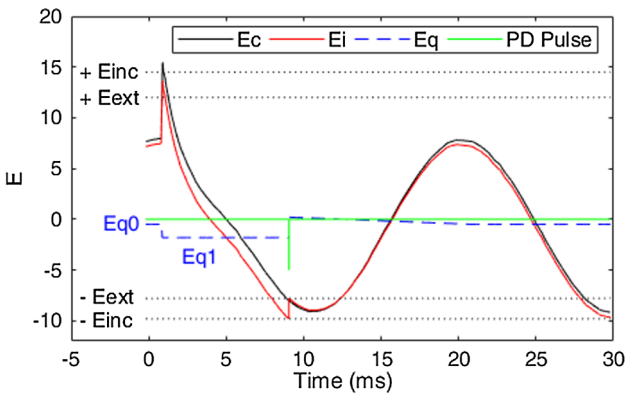


**Fig. 26.** The fields changes after 1st impulse in test 4 with charge decay.

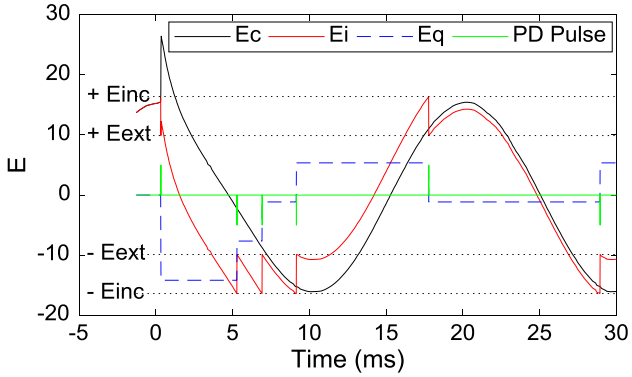


(a) With infinite first electron and no charge decay.

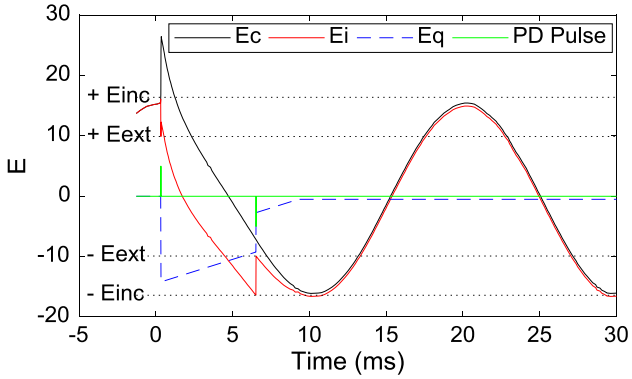


(b) With infinite first electron and charge decay.

**Fig. 27.** The fields changes after 5th impulse in test 7.

### 5.3. PDS initiate in the impulse period and persist at AC

In test 7, PD firstly initiated in the 5th impulse period, see Fig. 19. The explanation is similar to that in 5.2. Fig. 27 illustrates the field changes in this PD process.

When neglecting the charge decay between PD events, PD will be initiated by the impulse and then recur periodically, as shown in Fig. 27a. Fig. 27b shows the condition with considering the charge decay. After the negative PD, there is only a small number of charges left along the surface and in the traps, which contributes to $E_q$. After a

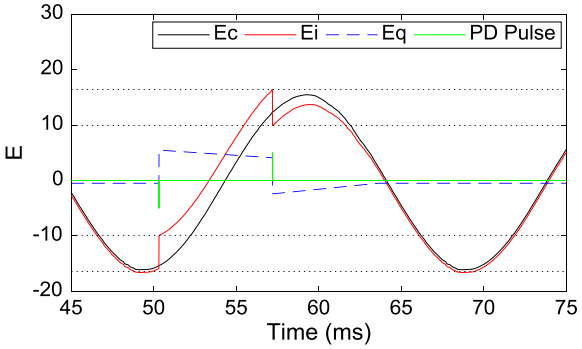


**Fig. 28.** The fields changes after 8th impulse in test 7.

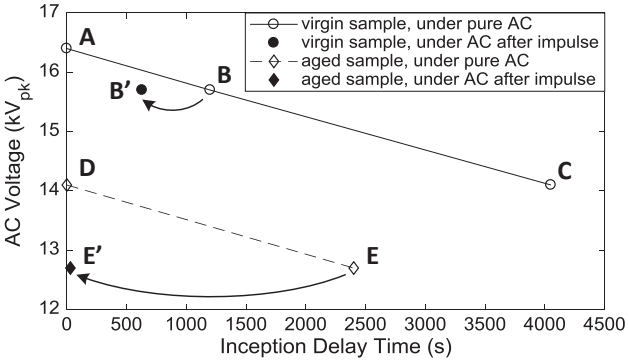


**Fig. 29.** The PD inception delay and time lag of cable sample 1.

short time, the residual surface charges all decay. A tiny $E_q$ is left, which is kept by the deposited charges in the traps. The detrapping process may take time, which will affect the PD activity in two ways. Firstly, the tiny $E_q$ causes an offset of $E_i$ from $E_c$. With this offset, $E_i$ may exceed $E_{inc}$, shown as the negative peak of $E_i$ in Fig. 27b. Secondly, there might be an absence of a free electron. In this case, even though $E_i$ exceeds $E_{inc}$, PD will not be ignited. This is why PD extinguished after the negative PD, as shown in Figs. 20 and 27b.

After the 8th impulse, PD initiated under AC voltage instead of being ignited in the impulse period. A negative PD initiated firstly and followed by a positive PD, then PD extinguished. A couple of milliseconds later, PD initiated and extinguished again in a same way. In general, PD recurred intermittently after the 8th impulse. This phenomenon is explained by the schematic in Fig. 28. Assuming the absence of a free electron, PD cannot be ignited even with $E_i$ exceeding $-E_{inc}$. At a certain moment, the electron deposited in the surface traps detraps successfully. When $E_i$ exceeds $-E_{inc}$ again, a negative PD ignites. Then $E_i$ follows $E_c$ with an offset of $E_q$, until it exceeds $E_{inc}$ in the positive cycle and causes a positive PD. After that, the decreased $E_i$ retracks $E_c$ with considering the charge decay until all the surface charges disappear. Then the same situation happens again as described in Fig. 27b. With absence of first electron, PD extinguishes with an exceeding $E_i$.

Such intermittent PD behaviours also happened after the 9th and 10th impulses. After the 9th impulse, PD initiated earlier, and the time interval between the intermittent PD events was shorter. After the 10th impulse, PD initiated even earlier and very soon they became sustained under AC voltage. PD can persist under AC voltage which is far below the inception voltage [15], provided the charges decay slowly as in the virgin defect, and there are always surface or deposited charges that generate $E_q$. From the previous analysis, the charges decay fast, and it may happen that all charges decay so that there is not a sufficient $E_q$ supporting $E_i$ to exceed $E_{inc}$. In this case, PD cannot persist under AC voltage anymore. Thus, the sustained PD might be explained by another reason.

Apart from the dimension and condition of the defects, the delay in PD inception also depends on the applied voltage [12], as shown in Eq. (2). With the same PDIV, a higher applied voltage will lead to a shorter time delay. According to [17], the strong increase of the time lag with decreasing field strength is due to the increase of the critical length, which restricts the active volume available for avalanche development. Wester et al. [31] presents the dependency between delay time and the applied 50 Hz voltage measured with different specimens. For each specimen, the delay time is considerably short for higher voltages and rather long for lower voltages. In the current work, $t_{delay}$ of cable sample 1 in virgin status was measured under 50 Hz AC voltages. The result is shown as the solid line with point A, B and C in Fig. 29. Point A indicates the PDIV, at which PD initiated with $t_{delay}$ of milliseconds and kept sustained. In test 7 where the AC voltage was 15.7 kV$_{pk}$, PD initiated and kept sustained after 10 impulses, i.e. around 630 s. However, according to Fig. 29, PD is supposed to initiate around 20 min after applying AC of 15.7 kV$_{pk}$, shown as point B. That is, the inception time lag under 15.7 kV$_{pk}$ decreased from $t_{delay}$ of 20 min to 630 s due to the application of impulses. This is shown as the point B switching to the point B′ in Fig. 29.

### 5.4. PDS initiate only at ac after the impulse

In test 5, PD initiated after 530 s of applying TV$_5$ with an AC voltage of 15.7 kV$_{pk}$, see Fig. 14. This means, a first electron was available at this moment, and the voltage of 15.7 kV$_{pk}$ was sufficient for PD to initiate. The delay time in this case is counted as the sum of 120 s under AC before the first impulse and 530 s under TV$_5$, i.e. 650 s, which can be regarded as point B' in Fig. 29 approximately.

After being stressed by more than two hundred impulses, the defect in cable sample 1 was supposed to be deteriorated. Thus, $t_{lag}$ of cable sample 1 was checked again under 50 Hz AC voltages, shown as the dash line in Fig. 29. The PDIV was measured as 14.1 kV$_{pk}$ with $t_{lag}$ of milliseconds, indicated as point D, which is decreased compared to that of virgin cable sample. At AC of 12.7 kV$_{pk}$, $t_{lag}$ was around 40 min, shown as point E. Test 6 was performed on the aged sample. When applying TV$_6$, PD did not initiate under 12.7 kV$_{pk}$ before the impulse but initiated three cycles after the impulse and kept sustained by the 12.7 kV$_{pk}$ AC. At this moment, the 12.7 kV$_{pk}$ AC was sufficient to initiate PD without time delay. In other words, $t_{lag}$ under 12.7 kV$_{pk}$ has decreased from 40 min to milliseconds, shown as point E switching to point E'.

### 5.5. Statistical analysis on the progress from pd initiation to sustained status

A single progress from PD initiation to intermittent recurrence and then to sustained status under impulse transients has been investigated in test 7. In test 8, such progress has been repeated for multiple times and the observations are analyzed with statistical techniques. In this way, we could statistically evaluate the effects of impulse transients on the PD progress.

The average pulse count distribution over time is applied to analyze the observations. The time base is determined as a 35-second period starting from the impulse moment. The pulse count distribution $H_n$ is determined as an array containing numbers of PD occurred in every second during the 35-second time base. The average pulse count distribution $H_n$' is the mean value of all the $H_n$ observed for $N$ impulses

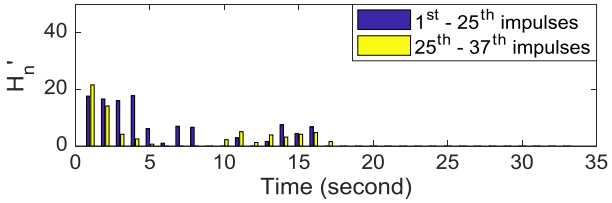


(a) PD pulse count distribution under $TV_{81}$ with 37 impulses.

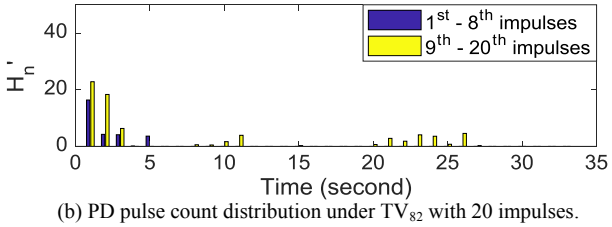


(b) PD pulse count distribution under $TV_{82}$ with 20 impulses.

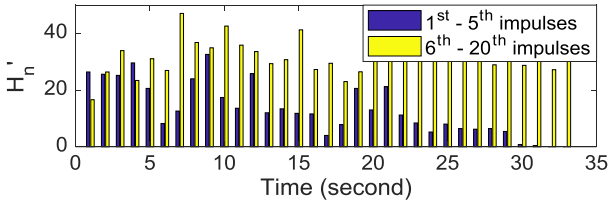


(c) PD pulse count distribution under $TV_{83}$ with 20 impulses.

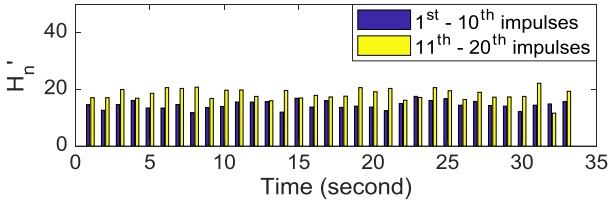


(d) PD pulse count distribution under $TV_{84}$ with 20 impulses.

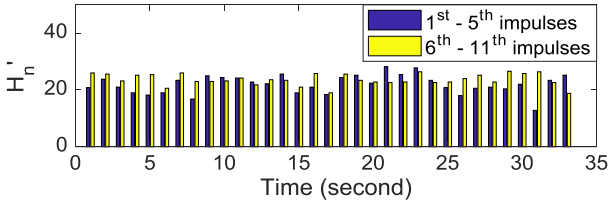


(e) PD pulse count distribution under $TV_{85}$ with 11 impulses.

**Fig. 30.** Statistical distribution of PD pulse count in test 8.

under the same testing voltage, as shown in Eq. (6).

$$H_n^{'} = \frac{\sum_{n=1}^{N} H_n}{N} \tag{6}$$

The PD repetition rate keeps at 1–2 PD per cycle during the entire test since the AC level of the testing voltages closely approximate PDIV. Therefore, a larger $H_n$' means PDs occur in more AC cycles, i.e. PD occurring more extensively. Fig. 30 shows the average pulse count distributions $H_n'$ over time under five testing voltages.

With $TV_{81}$ and $TV_{82}$, the AC levels are far below PDIV, the observations are shown in Fig. 30a and b. In Fig. 30a, during the first 25 impulses under $TV_{81}$, the initiated PD re-ignited intermittently and extinguished at last. Such PD behavior was also observed during the latter 12 impulses, i.e. the application of impulses had not affected the PD progress. The effect of impulses on PD rises up with $TV_{82}$, which is shown in Fig. 30b. During the first eight impulses, the initiated PD

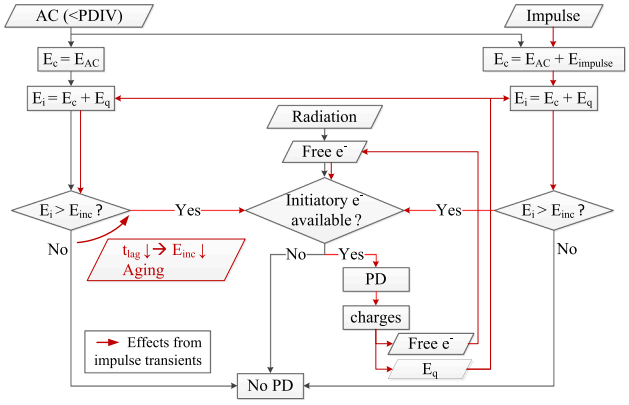


**Fig. 31.** The effects of impulse transients on PD.

extinguished fast within 10 s. With applying more impulses, during the 9th to 20th impulse, the initiated PD recurred more extended and extinguished after 30 s. This is due to the conductivity of the insulation surface caused by the accumulated damage. With more impulses being applied, more surface charges are accumulated. Consequently, the probability of PD initiating and recurring under AC becomes higher.

Fig. 30c shows the $H_n'$ under $TV_{83}$, whose AC level is closely approaching to PDIV. During the first five impulses, the initiated PD recurred with receding occurrence, then extinguished after 30 s. With more impulses being applied, during the 6th to 20th impulse, the initiated PDs were able to persist with the same occurrence extension. In this case, the initiated PDs transferred from an intermittent status to a sustained status. This can be explained as the decreasing of the inception time lag during the application of $TV_{83}$. With more impulses being applied, $t_{lag}$ under the AC of $TV_{83}$ has been decreased. Thus, the AC voltage became sufficient to ignite PD, which leads to the sustained PDs.

Under $TV_{84}$ and $TV_{85}$ where the AC levels exceed PDIV, impulses did not have a significant effect on PD behaviour. PDs were sustained all through the AC voltage, as shown in Fig. 30d and e.

## 6. Discussion

The different PD behaviour under impulse transients has been interpreted. Hereby, the effects of impulse transients on PD can be summarized as shown in Fig. 31.

With only AC voltage being applied on the cable, which is below PDIV, the local field is not sufficient for PD to initiate ($E_i < E_{inc}$, $E_q = 0$). When the impulse occurs, the background field in the defect $E_c$ is enhanced. This results in a very high local field $E_i$ which can ignite PD ($E_i > E_{inc}$, $E_q = 0$). Once the first electron generated by radiation is present, PD initiates. Those PDs always occur in the impulse periods. The charges created by PDs deposit along the insulation surface in the surface traps. Consequently, the surface charges become another source of the first electrons, and also generate a field $E_q$, which will superpose on the original $E_c$. The resulting $E_i$ may exceed $E_{inc}$ even after the impulse is gone. As a consequence, PDs will recur under only AC voltage ($E_i > E_{inc}$, $E_q \neq 0$). However, since PDEV is quite close to PDIV, the initiated PDs recur and extinguish intermittently.

The initiated PDs may also become sustained under AC voltage after the impulses. In that case, PDs are sustained by a sufficient electric field ($E_i > E_{inc}$), where the $E_{inc}$ is not the original one any more. The application of impulses leads to an accumulated strengthening of the electric field, and finally a shorter $t_{lag}$, i.e. a decreased $E_{inc}$. Moreover, it used to be the streamer breakdown taking place in the defect, with an inception voltage that is 5% higher than the Paschen curve. With the

defect being deteriorated by the impulses, Townsend breakdown starts to occur with the inception voltage being coincident with the Paschen curve [15]. As a result, the PDIV becomes lower than before, leading to $E_i$ above $E_{inc}$. Thus, the initiated PD can be sustained by the AC voltage.

## 7. Conclusions

In this paper, the PD behavior in artificial defects in MV XLPE cable samples under impulse transients were investigated. The cable was subjected to an AC voltage which was below PDIV without generating PD. With applying impulses, different scenarios of PD initiation and development have been observed:

- No PD could be initiated by the impulse transients.
- PDs were initiated by the impulses in the impulse period, and extinguished when the impulse was gone.
- PDs were initiated by the impulses in the impulse period. The initiated PDs recurred intermittently and persisted actively under AC voltage when the impulse was gone.
- PDs didn't initiate during the application of impulses but initiated under AC voltage when the impulse was gone.

These differences in PD behavior under impulse transients are related to the local electric field condition, the charges in the defects, and the aging status of the insulation:

- PD cannot initiate because the first electron is not available due to the stochastic generation of an electron by cosmic and background radiation.
- During the impulse moment, the local field $E_i$ is sufficient to initiate PD. When the impulse is gone, $E_i$ goes back to the original value which is not sufficient for PD initiation. And due to the charge decay, the field $E_q$ cannot contribute to enhance the field $E_i$. As a result, PD extinguishes.
- After the impulse, $E_q$ built up by the charges deposited in the insulator traps may stay and contribute to $E_i$. As soon as the first electron is available, PDs initiate again. This leads to the intermittent recurrence of PDs.
- The application of impulses would decrease $t_{lag}$. As a result, PDs can be sustained by AC voltage after the impulses.

Therefore, we conclude the effects of impulse transients on PDs:

- When there is at operating voltage a non-discharging defect existing in the cable, especially in the cable accessories, PD can be initiated by the impulse transients.
- Once PDs being initiated by the impulses, the generated surface charges will increase the probability of PD occurrence by contributing to the local field and providing free electrons.
- The application of multiple impulses may decrease the PD inception delay time or accelerate the aging process, which can both result in PD occurrence.

Moreover, a warning and a recommendation are given:

- The initiated PD may not lead to breakdown immediately, but may affect the degradation. In particularly, the PDIV may get decreased, which will cause more PD occurrence and accelerate the degradation. Moreover, such intermittent PDs can switch to sustained PDs, which threatens the cable insulation.
- Many PDs only occur at the impulse moment, which are difficult to be detected by the monitoring system. Therefore, a monitoring system which is able to measure PDs under an impulse transient within microseconds scale is recommended.

## Acknowledgment

Authors would like to thank TenneT B.V. of the Netherlands. for funding this project and providing technical support.

## References

[1] CIGRÉ WG B1.21. Third-party damage to underground and submarine cables. Technical Brochure 398, December 2009.
[2] Gulski E, Smit JJ, Wester FJ. PD knowledge rules for insulation condition assessment of distribution power cables. IEEE Trans Dielectr Electr Insul 2005;12(2):223–39.
[3] Gulski E, Wester FJ, Boone W, van Schaik N, Steennis EF, Groot ERS, et al. Knowledge rules support for CBM of power cable circuits. Cigre Session, 2002, paper 15-104.
[4] Abdolall K, Vandermaar AJ, Stephens M, Tarampi D. Effects of testing on service aged XLPE cables. In: 2015 IEEE electrical insulation conference (EIC); 2015. p. 93–7.
[5] Cao L, Grzybowski S. Accelerated aging study on 15 kV XLPE and EPR cables insulation caused by switching impulses. IEEE Trans Dielectr Electr Insul 2015;22(5):2809–17.
[6] Grzybowski S, Shrestha P, Cao L. Electrical aging phenomena of XLPE and EPR cable insulation energized by switching impulses. International conference on high voltage engineering and application. 2008. p. 422–5.
[7] Xu L, et al. The degradation of 10kV XLPE cable accessories under switching impulses. 2018 12th international conference on the properties and applications of dielectric materials (ICPADM). 2018. p. 463–6.
[8] Cao L, Zanwar A, Grzybowski S. Electrical aging phenomena of medium voltage EPR cable energized by ac voltage with switching impulses superimposed. IEEE electric ship technologies symposium. 2011. p. 353–6.
[9] Densley RJ, Salvage B. Partial discharges in gaseous cavities in solid dielectrics under impulse voltage conditions. IEEE Trans Electr Insul 1971;EI-6(2):54–62.
[10] Densley RJ. Partial discharges in electrical insulation under combined alternating and impulse stresses. IEEE Trans Electr Insul 1970;EI-5(4):96–103.
[11] Zhao XF, Yao X, Guo ZF, Wang YY, Li JH, Li YM. Partial discharge characteristics and mechanism in voids at impulse voltages. Meas Sci Technol 2011;22(3):035704.
[12] Niemeyer L. A generalized approach to partial discharge modeling. IEEE Trans Dielectr Electr Insul 1995;2(4):510–28.
[13] Gutfleisch F, Niemeyer L. Measurement and simulation of PD in epoxy voids. IEEE Trans Dielectr Electr Insul 1995;2(5):729–43.
[14] Morshuis PHF. Partial discharge mechanisms: Mechanisms leading to breakdown, analyzed by fast electrical and optical measurements, Ph.D. Thesis, Delft University Press, Delft, The Netherlands; 1993.
[15] Kreuger FH. Industrial high voltage-Vol. II. Delft, The Netherlands: Delft University Press; 1992.
[16] Gamez-Garcia M, Bartnikas R, Wertheimer MR. Synthesis reactions Involving XLPE Subjected to aartial discharges. IEEE Trans Electr Insul 1987;EI-22(2):199–205.
[17] Burgener H-, Frohlich K. Probability of partial discharge inception in small voids. 2001 annual report conference on electrical insulation and dielectric phenomena (Cat. No.01CH37225). 2001. p. 298–302.
[18] Zeller H-R, Baumann T, Cartier E, Dersch H, Pfluger P, Stucki F. The physics of electrical breakdown and prebreakdown in solid dielectrics. Festkörperprobleme. Berlin, Heidelberg: Springer; 1987. p. 223–40.
[19] Dissado LA, Fothergill JC. Electrical degradation and breakdown in polymers. IET; 1992.
[20] Eichhorn RM. Engineering dielectrics volume IIA electrical properties of solid insulating materials: molecular structure and electrical behavior. ASTM International; 1983.
[21] IEC 60270. High-voltage test techniques - Partial discharge measurements, March, 2001.
[22] IEC 60885-3. Electrical test methods for electric cables - Part 3: Test methods for partial discharge measurements on lengths of extruded power cables, June, 2015.
[23] Partial discharges software - PDflex: PD parameters and clustering. PDFlex - Unconventional partial discharge analysis. [Online]. Available: http://pdflex.tudelft.nl/. [Accessed: 28-Aug-2018].
[24] Rodrigo Mor A, Castro Heredia LC, Harmsen DA, Muñoz FA. A new design of a test platform for testing multiple partial discharge sources. Int J Electr Power Energy Syst 2018;94:374–84.
[25] Mor AR, Heredia LCC, Munoz FA. Estimation of charge, energy and polarity of noisy partial discharge pulses. IEEE Trans Dielectr Electr Insul 2017;24(4):2511–21.
[26] Mor AR, Morshuis PHF, Smit JJ. Comparison of charge estimation methods in partial discharge cable measurements. IEEE Trans Dielectr Electr Insul 2015;22(2):657–64.
[27] Chowdhuri P, et al. Review of research on nonstandard lightning voltage waves. IEEE Trans Power Deliv 1994;9(4):1972–81.
[28] Gulski E. Computer-aided recognition of partial discharges using statistical tools, Ph.D. Thesis, Delft University Press, Delft, The Netherlands; 1991.
[29] Hikita M, Yamada K, Nakamura A, Mizutani T, Oohasi A, Ieda M. Measurements of partial discharges by computer and analysis of partial discharge distribution by the Monte Carlo method. IEEE Trans Electr Insul 1990;25(3):453–68.
[30] Kreuger FH. Industrial High Voltage-Vol. I, Delft University Press, Delft, The Netherlands; 1991.
[31] Wester FJ, Guilski E, Smit JJ. Detection of partial discharges at different AC voltage stresses in power cables. IEEE Electr Insul Mag 2007;23(4):28–43.

**Jiayang Wu** was born in Nanjing, China in 1988. She received the BSc degree in electrical engineering from the Southeast University, Nanjing, China, in 2010, and the MSc degree in electrical power engineering from the RWTH Aachen University of Technology, Aachen, Germany in 2013. She is currently a Ph.D candidate in the Electrical Sustainable Energy Department at Delft University of Technology, Delft, The Netherlands. Her current research focuses on the effects of transients on the high voltage cable systems.

**Armando Rodrigo Mor** is an Industrial Engineer from Universitat Politècnica de València, in Valencia, Spain, with a Ph.D. degree from this university in electrical engineering. During many years he has been working at the High Voltage Laboratory and Plasma Arc Laboratory of the Instituto de Tecnología Eléctrica in Valencia, Spain. Since 2013 he is an Assistant Professor in the Electrical Sustainable Energy Department at Delft University of Technology, Delft, The Netherlands. His research interests include monitoring and diagnostic, sensors for high voltage applications, high voltage engineering, and HVDC.

**Johan J. Smit** is professor at the Delft University of Technology (The Netherlands) in High Voltage Technology and Management since 1996 and emeritus since 2015. After his graduation in experimental physics he received his PhD degree from Leiden University in 1979. After his research in cryogenic electromagnetism at the Kamerlingh Onnes Laboratory, he was employed as T&D research manager at KEMA's laboratories in Arnhem-NL for 20 years. Furthermore he was director of education in electrical engineering, supervisory board member of the power transmission company of South Holland, and CEO of the asset management foundation Ksandr for 10 years. In 2003 he was general chairman of the International Symposium on HV Engineering in Delft. He is TC-honorary member of CIGRE and past chairman of CIGRE D1 on Materials & Emerging Technologies. Currently he is convener of the area Substation Management for CIGRE B3 and he holds the international chair of Technical Committee IEC112 on Electrical Insulation Systems.